Contribution from the Laboratoire de Chimie des Métaux de Transition, E.R.A. au CNRS No. 608, Université Pierre et Marie Curie, 75230 Paris Cedex 05, France

Structural Study of Transition-Metal Hydride Complexes in Relation to Corrosion Inhibition: Crystal and Molecular Structures of $Ru_3H(CO)_{10}(SCH_2COOH)$ and $Ru_3H(CO)_9(C_7H_4NS_2)$

S. JEANNIN, Y. JEANNIN,* and G. LAVIGNE

Received December 21, 1977

The reaction of organic corrosion inhibitors (mercaptoethanoic acid, mercaptobenzothiazole) on $Ru_3(CO)_{12}$ has been undertaken under mild conditions. It leads to trinuclear hydrido complexes which have been characterized by ^1H NMR and X-ray diffraction studies. Both complexes $Ru_3H(CO)_{10}(SCH_2COOH)$ (I) and $Ru_3H(CO)_9(C_7H_4NS_2)$ (II) exhibit a high-field NMR proton resonance (I, τ 25.27; II, τ 22.8) which is consistent with a bridging hydride ligand. Complex I crystallizes in the monoclinic space group $P2_1/c$ with $a = 9.73 \pm 0.02$ Å, $b = 17.15 \pm 0.02$ Å, $c = 13.27 \pm 0.02$ Å, and $\beta = 118.06 \pm 0.1°$. The structure was solved by the heavy-atom method. Final discrepancy indices are $R_w = 0.049$ and $R = 0.053$. The ligand is coordinated through the bridging sulfur (Ru_1–S = Ru_2–S = 2.388 (6) Å) while the carboxylic group is not deprotonated. The stereochemical influence of the sulfur bridge is shown to favor the occurrence of the bridging hydride in a bent Ru–H–Ru system, without elongation of the metal–metal bond (Ru_1–Ru_2 = 2.839 (4) Å (hydrido bridged), Ru_1–Ru_3 = 2.839 (4) Å, Ru_2–Ru_3 = 2.826 (5) Å). Complex II crystallizes in the triclinic space group $P\bar{1}$ with $a = 10.29 \pm 0.002$ Å, $b = 11.21 \pm 0.02$ Å, $c = 9.74 \pm 0.02$ Å, $\alpha = 94.05 \pm 0.08°$, $\beta = 99.08 \pm 0.08°$, and $\gamma = 97.58 \pm 0.08°$. Final discrepancy indices are $R_w = 0.040$ and $R = 0.049$. The ligand molecule is coordinated to three metal atoms through the exocyclic bridging sulfur (S–Ru_1 = S–Ru_2 = 2.405 (5) Å) and through the thiazolic nitrogen atom (Ru_3–N = 2.177 (9) Å). The molecular structure of the ligand is discussed. Both complexes are proposed as stereochemical models of metal surface protection by organic inhibitors. In the case of complex II, such a model is checked by comparison of its infrared spectra with the reflection spectra obtained from the actual surface complex.

Introduction

The assumption of a surface complex is often postulated to explain the protective action of organic corrosion inhibitors on a metal surface.[1] In some cases, infrared multireflections may bring some interesting information on the ligand's coordination, but the actual structure of the complex is not known.

The analogy between clusters and metal surfaces which is used in heterogeneous catalysis[2] led us to undertake the preparation and structural study of some organometallic compounds as stereochemical models of corrosion inhibition. The value of such models was then checked by comparison of their infrared spectra with the corresponding reflection spectra obtained on the actual surface complex.[3]

This work concerns two sulfur-containing ligands, mercaptoethanoic acid and mercaptobenzothiazole, in which a possible competition between several donor atoms may occur. The choice of $Ru_3(CO)_{12}$ as metal support was previously discussed,[4] the main point being the retention of the metal triangle. The first investigation was the reaction of mercaptobenzothiazole; it led to mononuclear and dinuclear species.[4,5] The conditions required to avoid the breakdown of the cluster were found for mercaptoethanoic acid and afforded the trinuclear species $Ru_3H(CO)_{10}(SCH_2COOH)$, in agreement with the model proposed by Lewis and co-workers for closely related thiol derivatives.[6] The same reaction conditions were then applied to mercaptobenzothiazole, leading to a new complex with unusual stoichiometry: $Ru_3H(CO)_9(C_7H_4NS_2)$. From NMR and X-ray diffraction studies, these compounds are shown to be closely related to the series of hydrido carbonyl complexes recently reviewed by Churchill and co-workers.[7] In spite of the different carbonyl stoichiometries of both complexes, the thiol and thioamide groups are shown to have the same action on the metal. Both complexes are also new examples of noncorrelation between M–M distance and M–H–M bonding.

Experimental Section

Preparation of the Complexes. (a) $Ru_3H(CO)_{10}(SCH_2COOH)$. The experimental conditions described by Lewis for thiol reaction on $Ru_3(CO)_{12}$[6] cannot be used with mercaptoethanoic acid which requires very mild conditions; the reaction was carried out under nitrogen dried on P_4O_{10}. $Ru_3(CO)_{12}$ (300 mg) was dissolved in 25 mL of air-free toluene. A 0.05-mL volume of mercaptoethanoic acid was then added. The mixture was kept at 50 °C for 1 h (higher temperatures rapidly result in breakdown of the metal triangle). The orange solution was then cooled, and 60 mg of orange air-stable crystals was obtained. They are suitable for X-ray analysis but can be recrystallized from a tetrahydrofuran–toluene mixture. The high density of crystals (2.2) and their infrared spectra suggested the formation of a complex.

(b) $Ru_3H(CO)_9(C_7H_4NS_2)$. Red crystals were obtained from 300 mg of $Ru_3(CO)_{12}$ and 80 mg of mercaptobenzothiazole, using the same experimental conditions. Crystallization required several days, at a temperature of ca. −20 °C.

In both cases, the formulation of the complexes was found from a crystal structure determination.

Infrared Spectra. IR spectra were recorded on Perkin-Elmer 283 spectrophotometer. Free ligand and complexes were sampled as KBr pellets.

NMR Spectra. The NMR spectra were recorded on a Varian XL 100. A single high-field proton resonance was observed in both cases: $Ru_3H(CO)_{10}(SCH_2COOH)$, τ 25.27; $Ru_3H(CO)_9(C_7H_4NS_2)$, τ 22.8. This is consistent with the presence of a bridging hydride ligand.[6]

X-ray Diffraction Studies. (a) $Ru_3H(CO)_{10}(SCH_2COOH)$. The crystal selected for X-ray analysis was prismatic (0.10 × 0.16 × 0.12 mm). Preliminary Laue and precession photographs showed the unit cell to be monoclinic. Lattice constants were obtained from film micrometering and diffractometer alignments and are as follow: space group $P2_1/c$, $a = 9.53 \pm 0.02$ Å, $b = 17.15 \pm 0.02$ Å, $c = 13.27 \pm 0.02$ Å, $\beta = 118.6 \pm 0.1°$. The crystal was set up on a 300-mm Eulerian cradle, the ϕ axis being collinear with the c axis.

Data collection was made on an automatic diffractometer built in the laboratory: radiation, Mo Kα; takeoff angle, 3°; collimator, ϕ = 0.4 mm; length, 150 mm; crystal–focus distance, 230 mm; crystal–counter distance, 230 mm; detector aperture, ϕ 2 mm; scan type, θ–2θ coupled, at a rate of 1.1°/min in θ; scan length, ca. 1°, taking $\Delta\lambda/\lambda$ into account. The graphite monochromator was set in front of the counter window, and the scintillation counter and pulse height analyzer were set on Mo Kα energy in such a way that 90% of the intensity was collected. A total of 3238 independent reflections, including 215 zeros, were collected at room temperature, up to $(\sin\theta)/\lambda = 0.594$ Å^{-1}. The reflections 060, 004, and 400 were measured as standards, every 50 reflections, and a linear intensity decay of 6.7% was observed during data collection.

Treatment of Intensity Data. Intensities were first corrected from Lorentz and polarization factors. Other corrections (standard decay, absorption) were applied only at the end of the refinement to check their effect on R improvement. Atomic form factors were taken from

0020-1669/78/1317-2103$01.00/0

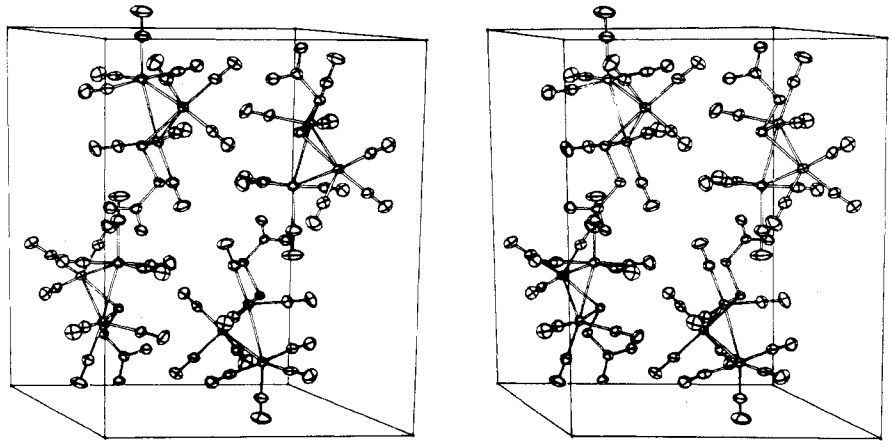

Figure 1. Stereoscopic view showing molecular packing of $Ru_3H(CO)_{10}(SCH_2COOH)$ within the unit cell.

Cromer and Mann,[8] including $\Delta f'$ and $\Delta f''$. For every observed structure factor (F_o), a standard deviation was computed as $\sigma = \Delta I/2F_o$, where I is the integrated intensity and ΔI its statistical error. A different σ was computed for "unobserved" reflections, $\sigma = (\Delta I/3)^{1/2}$, when $I < \Delta I$.

Structure refinements were made by full-matrix least squares, minimizing the weighted function R_w, $R_w = [\Sigma w(|F_o| - |F_c|)^2/\Sigma w \cdot |F_o|^2]^{1/2}$, with $w = 1/\sigma^2$; the nonweighted function was $R = \Sigma||F_o| - |F_o||/\Sigma|F_o|$.

A three-dimensional Patterson map was found to be consistent with a triangular array of Ru atoms. All other nonhydrogen atoms were found on a subsequent Ru-phased F_o Fourier synthesis. Refinement of their coordinates, using isotropic temperature factors, gave convergence at $R_w = 0.081$. The introduction of anisotropic thermal parameters followed by three cycles of full-matrix refinement dropped R_w to 0.051. At this step, the observed structure factors were corrected for standard decay ($R_w \rightarrow 0.050$) and for absorption ($\mu = 25$ cm^{-1}; maximum and minimum transmission factors were 0.772 and 0.645, respectively). The last correction gave no significant improvement in R_w. An electron density difference map was then calculated (excluding 215 unobserved reflections), in order to locate hydrogen atoms. The highest peaks were found to be the hydrogen atoms of the ligand: H_1 at 0.97 e/Å^3 and H_2 at 0.88 e/Å^3 (CH_2 group); H_3 at 0.85 e/Å^3 (carboxylic group). This confirmed that the carboxylic group was not deprotonated. Since the NMR spectra gave evidence of a hydride ligand, we were also interested in its location.

Although the best information on some M–H–M bonds has been obtained from neutron diffraction,[9] some X-ray structure determinations recently have led to a direct location of such a hydride ligand.[7,10–15] These publications mentioned the method proposed by Ibers and LaPlaca,[16] in which decreasing $(\sin\theta)/\lambda$ limits were used to enhance hydrogen atoms in difference Fourier maps. It was shown that if a peak is an artifact, it would shift or disappear as the number of terms is varied, while the electron density of hydrogen atoms would remain in the same place. However, caution must presently be exercised because the hydrogen atom is "buried" in the metal orbitals. In our case, the difference map using the whole data set showed up a residue of 0.7 e/Å^3 between Ru_1 and Ru_2, approximately trans to the carbonyl ligands $C_{13}O_{13}$ and $C_{23}O_{23}$. Successive Fourier maps with decreasing limits 0.33 and 0.25 showed that this residue had the same behavior as the other hydrogen atoms, H_1, H_2, and H_3, of the ligand: (1) no displacement was observed, (2) the volume of the four peaks was increased, and (3) the four residues were significantly enhanced in the same way as shown in the following table; the sharp decrease of the number of terms is in the ratio $3015/554 \approx 5.5$ while residues are only reduced to half of their value.

	H_1	H_2	H_3	Hydride?
Whole data excluding zeros (3015 observns)	0.97	0.88	0.85	0.70
Limited data (0.33) excluding zeros (554 observns)	0.55	0.43	0.41	0.34

This result led us to consider that the observed residue might belong to the hydride ligand. Doubt concerning the validity of this peak arose from the presence of a residue (0.6 e/Å^3 on a metal–carbon bond) which could be attributed to an improper treatment of metal scattering.

Therefore, only the hydrogen atoms of the ligand were introduced in the refinement. The anisotropic thermal parameters of C_1 and O_2 were respectively imposed to H_1, H_2, and H_3. Refinement led to $R_w = 0.049$ and $R = 0.059$. The difference between the two values was attributed to the influence of the weak and zero reflections. Indeed, after elimination of reflections with $F_o < 3\sigma$, the refinement with 2908 observations led to $R_w = 0.049$ and $R = 0.053$. It is noteworthy that the final coordinates were found identical in both cases, within experimental error. Considering the satisfactory adjustment between F_o and F_c at low diffraction angles, it was not found necessary to use a secondary extinction parameter.

Final atomic coordinates and anisotropic thermal parameters are reported in Tables I and II, with their estimated standard deviations in parentheses. Interatomic distances and bond angles (Tables III and IV) were computed with the program ORFFE. The reported values are not corrected for thermal vibrations. Several views of the molecule (Figures 1, 2, 3, and 4) were made with the program ORTEP.[17] A list of observed and calculated structure factors is available as supplementary material.

(b) $Ru_3H(CO)_9(C_7H_4NS_2)$. The crystal selected was prismatic (0.10 × 0.10 × 0.07 mm). It was set up along the $h0\bar{h}$ axis. Preliminary

Table I. Final Atomic Coordinates in $Ru_3H(CO)_{10}(SCH_2COOH)$ with Esd's in Parentheses

Ru_1	0.62087 (8)	0.27291 (4)	0.69989 (6)
Ru_2	0.86307 (8)	0.17315 (4)	0.70676 (6)
Ru_3	0.62674 (9)	0.11282 (4)	0.75625 (6)
S	0.8922 (2)	0.2671 (1)	0.8483 (2)
C_{11}	0.415 (1)	0.2627 (6)	0.5694 (8)
O_{11}	0.2906 (9)	0.2608 (5)	0.4929 (7)
C_{12}	0.628 (1)	0.3784 (6)	0.6522 (8)
O_{12}	0.615 (1)	0.4403 (5)	0.6172 (8)
C_{13}	0.532 (1)	0.2897 (5)	0.7991 (8)
O_{13}	0.485 (1)	0.2996 (5)	0.8599 (7)
C_{21}	0.789 (1)	0.1058 (5)	0.5786 (9)
O_{21}	0.741 (1)	0.0677 (4)	0.4980 (7)
C_{22}	1.021 (1)	0.2229 (5)	0.6743 (7)
O_{22}	1.117 (1)	0.2495 (4)	0.6626 (7)
C_{23}	1.007 (1)	0.0985 (6)	0.8144 (9)
O_{23}	1.088 (1)	0.0544 (5)	0.8774 (8)
C_{31}	0.494 (1)	0.0985 (5)	0.590 (1)
O_{31}	0.414 (1)	0.0864 (4)	0.4977 (7)
C_{32}	0.447 (1)	0.1121 (5)	0.7808 (9)
O_{32}	0.339 (1)	0.1121 (5)	0.8007 (8)
C_{33}	0.693 (1)	0.0028 (6)	0.778 (1)
O_{33}	0.725 (1)	−0.0588 (5)	0.793 (1)
C_{34}	0.772 (1)	0.1324 (6)	0.9168 (9)
O_{34}	0.853 (1)	0.1358 (5)	1.0138 (7)
C_1	1.000 (1)	0.3512 (4)	0.8324 (7)
H_1	0.94 (1)	0.355 (7)	0.74 (1)
H_2	1.09 (1)	0.335 (7)	0.84 (1)
C_2	1.001 (1)	0.4161 (5)	0.9047 (8)
O_1	0.9210 (9)	0.4768 (3)	0.8606 (5)
O_2	1.0860 (8)	0.4069 (4)	1.0146 (5)
H_3	1.19 (2)	0.399 (8)	1.01 (1)

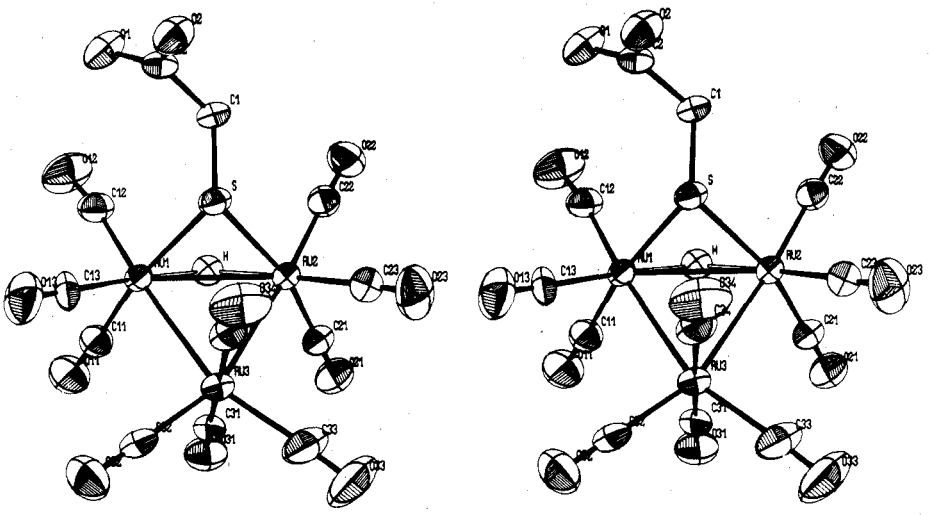

Figure 2. Stereoscopic view of the molecule $Ru_3H(CO)_{10}(SCH_2COOH)$ (ORTEP diagram with 50% probability ellipsoids; the hydride ligand has been represented with a dummy ellipsoid).

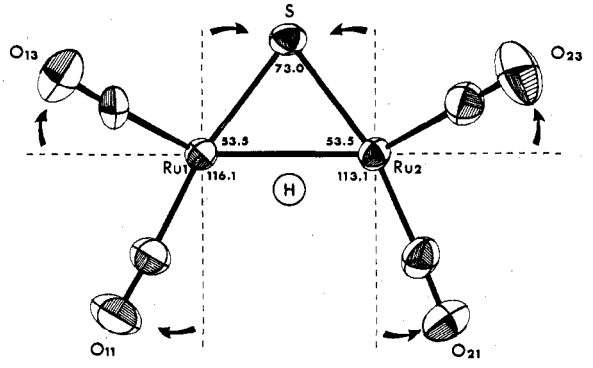

Figure 3. Stereochemical influence of the sulfur bridge.

Table II. Anisotropic Thermal Parameters[a] in $Ru_3H(CO)_{10}(SCH_2COOH)$

Atom	B_{11}	B_{22}	B_{33}	B_{12}	B_{13}	B_{23}
Ru_1	2.54 (3)	2.14 (3)	2.83 (3)	0.02 (2)	1.08 (2)	−0.28 (2)
Ru_2	2.63 (3)	2.16 (3)	3.05 (3)	−0.02 (2)	1.32 (2)	−0.27 (2)
Ru_3	3.17 (3)	2.37 (3)	3.48 (3)	−0.38 (2)	1.64 (3)	0.14 (2)
S	2.91 (9)	2.31 (8)	2.76 (8)	−0.32 (7)	1.04 (7)	−0.26 (7)
C_{11}	2.8 (4)	3.5 (4)	3.6 (4)	−0.0 (3)	0.9 (4)	−0.2 (4)
O_{11}	3.2 (3)	6.0 (5)	5.1 (4)	0.0 (3)	0.2 (3)	−0.3 (4)
C_{12}	3.5 (4)	3.2 (4)	3.6 (4)	−0.5 (3)	1.2 (4)	−0.3 (4)
O_{12}	8.3 (6)	3.1 (4)	6.5 (5)	0.0 (4)	2.3 (4)	1.5 (4)
C_{13}	2.7 (4)	3.9 (5)	4.0 (4)	1.0 (3)	2.0 (4)	−0.0 (4)
O_{13}	6.5 (5)	6.1 (5)	5.5 (4)	1.1 (4)	3.7 (4)	−1.2 (4)
C_{21}	3.9 (5)	2.5 (4)	4.7 (5)	−0.2 (3)	2.3 (4)	−0.6 (4)
O_{21}	5.5 (4)	4.1 (4)	5.2 (4)	−0.3 (3)	2.5 (3)	−1.5 (3)
C_{22}	3.2 (4)	3.5 (4)	3.2 (4)	−0.1 (4)	1.5 (3)	−0.6 (3)
O_{22}	4.1 (4)	5.0 (4)	5.5 (4)	−0.6 (3)	2.8 (3)	−0.4 (3)
C_{23}	3.5 (5)	3.2 (4)	4.3 (5)	0.1 (4)	1.9 (4)	−0.3 (4)
O_{23}	5.3 (5)	6.1 (5)	6.4 (5)	2.5 (4)	2.5 (4)	3.0 (4)
C_{31}	3.0 (4)	2.7 (4)	5.2 (6)	−0.4 (3)	2.0 (4)	0.1 (4)
O_{31}	4.6 (4)	4.7 (4)	4.0 (4)	−1.1 (3)	1.4 (3)	−0.5 (3)
C_{32}	4.3 (5)	1.9 (4)	6.1 (6)	−0.6 (3)	2.4 (5)	−0.3 (4)
O_{32}	4.8 (5)	6.2 (5)	8.5 (6)	0.1 (4)	4.5 (4)	0.8 (4)
C_{33}	6.0 (7)	2.8 (5)	5.6 (6)	−0.6 (4)	2.1 (5)	−0.5 (4)
O_{33}	9.9 (8)	2.8 (4)	10.0 (8)	1.3 (4)	2.8 (6)	−0.1 (4)
C_{34}	4.9 (5)	2.8 (4)	4.5 (5)	−0.5 (4)	2.6 (5)	−0.3 (4)
O_{34}	7.2 (5)	5.7 (4)	4.3 (4)	−1.6 (4)	2.2 (4)	−0.2 (3)
C_1	3.0 (4)	2.4 (4)	2.8 (4)	−0.4 (3)	1.4 (3)	−0.3 (3)
C_2	2.9 (4)	2.6 (4)	3.3 (4)	−0.8 (3)	1.5 (3)	−0.1 (3)
O_1	5.7 (4)	2.5 (3)	3.1 (3)	0.3 (3)	1.2 (3)	−0.3 (2)
O_2	4.3 (3)	3.1 (3)	3.1 (3)	0.3 (2)	1.0 (3)	−0.1 (2)

[a] These anisotropic thermal parameters have units of A^2. They enter the expression for the structure factor in the form $\exp[-0.25(B_{11}h^2a^{*2} + B_{22}k^2b^{*2} + B_{33}l^2c^{*2} + 2B_{12}hka^*b^* + 2B_{13}hla^*c^* + 2B_{23}klb^*c^*)]$.

Table III. Interatomic Distances in $Ru_3H(CO)_{10}(SCH_2COOH)$ with Esd's in Parentheses (A)

	Metal-Metal Bonds		
Ru_1-Ru_2	2.839 (4)	Ru_2-Ru_3	2.827 (5)
Ru_1-Ru_3	2.839 (4)		
	Metal-Ligand Bonds		
Ru_1-S	2.387 (6)	Ru_2-S	2.388 (3)
	Bonds Involving Ligand Atoms		
S-C_1	1.842 (8)	C_1-H_1	1.1 (1)
C_1-C_2	1.47 (1)	C_1-H_2	0.9 (1)
C_2-O_1	1.26 (1)	O_2-H_3	0.9 (1)
C_2-O_2	1.29 (1)		
	Bonds Involving Axial Carbonyls		
Ru_1-C_{11}	1.90 (1)	C_{11}-O_{11}	1.14 (1)
Ru_2-C_{21}	1.89 (1)	C_{21}-O_{21}	1.15 (1)
Ru_3-C_{31}	1.95 (1)	C_{31}-O_{31}	1.12 (1)
Ru_3-C_{34}	1.93 (1)	C_{34}-O_{34}	1.14 (1)
	Bonds Involving Equatorial Carbonyls		
Ru_1-C_{12}	1.93 (1)	C_{12}-O_{12}	1.14 (1)
Ru_1-C_{13}	1.90 (1)	C_{13}-O_{13}	1.11 (1)
Ru_2-C_{22}	1.95 (1)	C_{22}-O_{22}	1.10 (1)
Ru_2-C_{23}	1.92 (1)	C_{23}-O_{23}	1.12 (1)
Ru_3-C_{32}	1.82 (1)	C_{32}-O_{32}	1.18 (1)
Ru_3-C_{33}	1.97 (1)	C_{33}-O_{33}	1.09 (1)

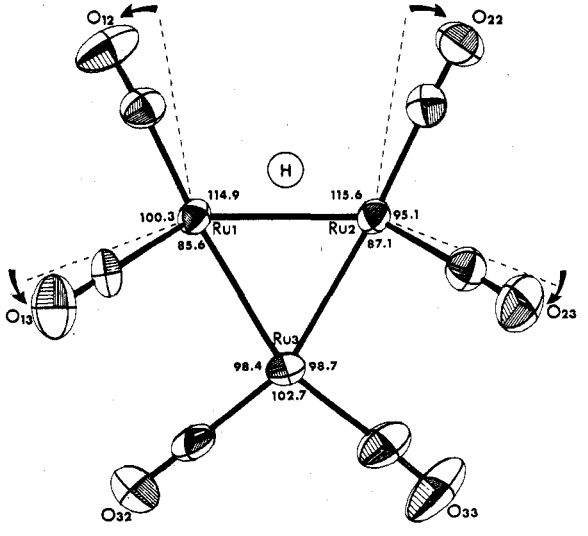

Figure 4. Stereochemical influence of the bridging hydride: equatorial distribution of carbonyl ligands in $Ru_3H(CO)_{10}(SCH_2COOH)$ with respect to $Ru_3(CO)_{12}$.

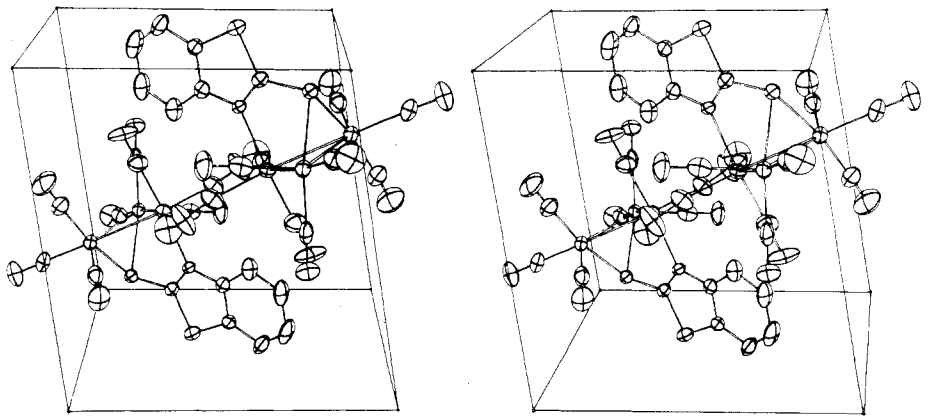

Figure 5. Stereoscopic view showing molecular packing of $Ru_3H(CO)_9(C_7H_4NS_2)$ within the unit cell.

Table IV. Principal Bond Angles in $Ru_3H(CO)_{10}(SCH_2COOH)$ with Esd's in Parentheses (deg)

	Metal Triangle Angles		
Ru_2-Ru_1-Ru_3	59.7 (1)	Ru_2-Ru_3-Ru_1	60.1 (1)
Ru_1-Ru_2-Ru_3	60.1 (1)		
	Sulfur Bridge Angles		
Ru_1-S-Ru_2	73.0 (1)	S-Ru_2-Ru_1	53.5 (1)
S-Ru_1-Ru_2	53.5 (1)		
	Ligand Angles		
Ru_1-S-C_1	108.4 (3)	C_1-C_2-O_1	120.7 (8)
Ru_2-S-C_1	107.4 (3)	C_1-C_2-O_2	116.5 (8)
S-C_1-C_2	110.4 (6)	O_1-C_2-O_2	122.7 (8)
	Metal Surrounding Angles		
S-Ru_1-Ru_2	53.5 (1)	C_{11}-Ru_1-C_{12}	88.4 (4)
S-Ru_1-Ru_3	82.29 (7)	C_{11}-Ru_1-C_{13}	92.2 (4)
S-Ru_1-C_{12}	96.5 (3)	C_{12}-Ru_1-C_{13}	100.3 (4)
S-Ru_1-C_{13}	95.7 (3)	C_{13}-Ru_1-Ru_3	85.6 (3)
C_{11}-Ru_1-Ru_2	116.2 (3)	C_{12}-Ru_1-Ru_2	114.9 (3)
C_{11}-Ru_1-Ru_3	91.8 (3)		
S-Ru_2-Ru_1	53.5 (1)	C_{21}-Ru_2-C_{22}	93.6 (4)
S-Ru_2-Ru_3	82.5 (1)	C_{21}-Ru_2-C_{23}	95.0 (4)
S-Ru_2-C_{22}	93.8 (3)	C_{22}-Ru_2-C_{23}	95.06 (4)
S-Ru_2-C_{23}	95.3 (3)	C_{23}-Ru_2-Ru_3	87.1 (3)
C_{21}-Ru_2-Ru_1	113.1 (3)	C_{22}-Ru_2-Ru_1	115.6 (3)
C_{21}-Ru_2-Ru_3	89.4 (3)		
C_{34}-Ru_3-Ru_1	92.1 (3)	C_{31}-Ru_3-C_{32}	92.3 (5)
C_{34}-Ru_3-Ru_2	87.9 (3)	C_{31}-Ru_3-C_{33}	92.0 (5)
C_{34}-Ru_3-C_{32}	92.4 (5)	Ru_1-Ru_3-C_{32}	98.4 (3)
C_{34}-Ru_3-C_{33}	89.6 (5)	C_{32}-Ru_3-C_{33}	102.7 (5)
C_{31}-Ru_3-Ru_1	84.6 (3)	C_{33}-Ru_3-Ru_2	98.7 (4)
C_{31}-Ru_3-Ru_2	86.8 (3)		

precession photographs showed the unit cell to be triclinic (space group $P\bar{1}$), with the following parameters: $a = 10.29 \pm 0.02$ Å, $b = 11.21 \pm 0.02$ Å, $c = 9.74 \pm 0.02$ Å, $\alpha = 94.05 \pm 0.08°$, $\beta = 99.08 \pm 0.08°$, $\gamma = 97.58 \pm 0.08°$.

Data collection conditions were the same as those described above. A total of 3060 independent reflections were collected at room temperature, up to $(\sin\theta)/\lambda = 0.55$ Å^{-1}. A slight decrease in intensity (ca. 4%) was observed and corrected, using $60\bar{6}$, 006, and 040 as standards. Scattering factors for neutral Ru, S, O, N, and C atoms were taken from Cromer and Mann,[8] including real and imaginary terms of anomalous dispersion.

The structure was solved by the heavy-atom method. A three-dimensional Patterson map confirmed the retention of the metal triangle. A Ru-phased F_o synthesis gave then evidence of the ligand molecule and nine carbonyl groups. Full-matrix least-squares refinement converged to an R_w of 0.11 with isotropic temperature factors. Anisotropic thermal parameters were then introduced. The coordinates of the four hydrogen atoms of the benzene ring were then computed from the program FINDH. In a first step, these atoms were constrained to the same variations as the carbon atoms to which they were bound. Five cycles of full-matrix least-squares refinement led to $R_w = 0.044$ and $R = 0.074$. The important difference between the two values was assigned to the bad influence of weak and zero reflections which were numerous in the data. Therefore, the final refinement (including hydrogen coordinates) was made for 2374 data ($F_o > 3\sigma$) and resulted in $R_w = 0.040$ and $R = 0.049$. At this final step, a difference Fourier synthesis was computed for a careful search of the hydride ligand. The highest peak in the map (0.8 e/Å^3) was found to complete the octahedron surrounding Ru_1 and Ru_2 (it was trans to $C_{13}O_{13}$ and $C_{23}O_{23}$). As observed in the previous structure, decreasing $(\sin\theta)/\lambda$ limits were found to enhance the peak which remained in the same place. However, its large area suggested that it was also receiving contributions of artifacts resulting from an improper treatment of metal scattering. Following these observations, it was not found reasonable to refine the hydride coordinates. In our ORTEP views (Figures 5, 6, 7, and 8) it was, however, represented (with a dummy ellipsoid) in the mean plane (C_{13}–Ru_1–Ru_2–C_{23}), at a distance of ca. 1.85 Å of both metal atoms.

Table V. Atomic Coordinates in $Ru_3H(CO)_9(C_7H_4NS_2)$ with Esd's in Parentheses

Atom	x	y	z
Ru_1	0.2928 (1)	0.02484 (9)	0.18463 (9)
Ru_2	0.2417 (1)	0.21802 (9)	0.02068 (9)
Ru_3	0.36405 (9)	0.26339 (9)	0.30051 (9)
S_1	0.0828 (3)	0.0978 (3)	0.1296 (3)
C_1	0.069 (1)	0.1857 (9)	0.278 (1)
N	0.1675 (8)	0.2538 (8)	0.3589 (9)
S_2	−0.0849 (3)	0.1899 (3)	0.3290 (3)
C_2	−0.007 (1)	0.291 (1)	0.472 (1)
C_3	0.129 (1)	0.3136 (9)	0.472 (1)
C_4	0.211 (1)	0.393 (1)	0.578 (1)
H_4	0.33 (2)	0.43 (1)	0.59 (1)
C_5	0.148 (2)	0.442 (1)	0.676 (1)
H_5	0.18 (2)	0.47 (2)	0.72 (1)
C_6	0.017 (3)	0.421 (1)	0.676 (2)
H_6	−0.08 (2)	0.41 (2)	0.68 (2)
C_7	−0.063 (2)	0.343 (2)	0.577 (2)
H_7	−0.15 (2)	0.33 (2)	0.57 (2)
C_{11}	0.473 (2)	0.001 (1)	0.203 (1)
O_{11}	0.581 (1)	−0.012 (1)	0.216 (1)
C_{12}	0.223 (1)	−0.134 (1)	0.090 (1)
O_{12}	0.192 (1)	−0.234 (1)	0.045 (1)
C_{13}	0.276 (1)	−0.013 (1)	0.369 (1)
O_{13}	0.268 (1)	−0.040 (1)	0.477 (1)
C_{21}	0.390 (1)	0.295 (1)	−0.049 (1)
O_{21}	0.479 (1)	0.342 (1)	−0.084 (1)
C_{22}	0.152 (1)	0.157 (1)	−0.168 (1)
O_{22}	0.102 (1)	0.128 (1)	−0.281 (1)
C_{23}	0.180 (1)	0.368 (1)	0.043 (1)
O_{23}	0.136 (1)	0.457 (1)	0.057 (1)
C_{31}	0.528 (1)	0.268 (1)	0.236 (1)
O_{31}	0.627 (1)	0.273 (1)	0.201 (1)
C_{32}	0.442 (1)	0.227 (1)	0.486 (1)
O_{32}	0.501 (1)	0.206 (1)	0.584 (1)
C_{33}	0.381 (1)	0.435 (1)	0.320 (1)
O_{33}	0.390 (1)	0.540 (1)	0.336 (1)

Final atomic coordinates and anisotropic thermal parameters are reported in Tables V and VI. Interatomic distances and bond angles are in Tables VII and VIII. A list of observed and calculated structure

Table VI. Anisotropic Thermal Parameters[a] in $Ru_3H(CO)_9(C_7H_4NS_2)$

Atom	B_{11}	B_{22}	B_{33}	B_{12}	B_{13}	B_{23}
Ru_1	3.83 (5)	3.88 (5)	2.94 (4)	0.92 (4)	0.64 (4)	0.25 (4)
Ru_2	3.92 (5)	4.32 (5)	2.87 (4)	0.91 (4)	0.94 (3)	0.57 (4)
Ru_3	2.73 (4)	4.16 (5)	3.54 (4)	−0.01 (4)	0.32 (3)	0.11 (4)
S_1	3.0 (1)	4.4 (1)	3.0 (1)	0.3 (1)	0.4 (1)	−0.2 (1)
C_1	3.0 (5)	3.3 (5)	3.4 (5)	0.3 (4)	1.1 (4)	0.5 (4)
N	2.2 (4)	4.5 (4)	2.9 (4)	0.5 (4)	0.6 (3)	−0.0 (3)
S_2	3.0 (1)	7.0 (2)	4.6 (2)	0.8 (1)	1.2 (1)	0.4 (1)
C_2	4.4 (6)	5.4 (6)	3.2 (5)	2.3 (5)	1.1 (5)	1.3 (5)
C_3	4.3 (6)	2.9 (5)	3.2 (5)	1.0 (4)	1.0 (4)	0.9 (4)
C_4	7.3 (8)	3.0 (5)	4.0 (6)	0.1 (5)	0.8 (6)	−0.3 (5)
C_5	10. (1)	4.7 (8)	3.9 (7)	1.4 (8)	1.2 (7)	−1.1 (6)
C_6	13. (2)	7. (1)	6. (1)	6. (1)	5. (1)	1.0 (8)
C_7	6.7 (9)	6.1 (8)	4.6 (7)	3.0 (7)	3.0 (7)	1.6 (7)
C_{11}	7.0 (8)	4.1 (6)	2.4 (4)	2.3 (6)	0.8 (5)	−0.1 (4)
O_{11}	5.4 (6)	10.3 (8)	7.0 (6)	4.1 (5)	1.4 (5)	0.8 (5)
C_{12}	5.8 (8)	5.1 (7)	4.4 (6)	2.0 (6)	0.7 (5)	0.5 (5)
O_{12}	9.2 (7)	4.8 (5)	9.3 (7)	0.9 (5)	0.8 (6)	−1.2 (5)
C_{13}	4.3 (6)	2.4 (5)	5.5 (7)	−0.5 (4)	0.3 (5)	0.1 (5)
O_{13}	8.9 (7)	8.4 (7)	4.1 (5)	−1.3 (5)	2.1 (5)	2.0 (5)
C_{21}	5.3 (8)	6.8 (9)	5.4 (7)	1.0 (7)	2.3 (6)	0.2 (6)
O_{21}	7.4 (7)	13. (1)	11.1 (7)	−1.6 (7)	5.1 (7)	3.0 (8)
C_{22}	6.5 (8)	4.7 (6)	3.2 (6)	0.4 (5)	1.7 (5)	0.3 (5)
O_{22}	10.0 (7)	5.7 (5)	4.0 (4)	−0.4 (5)	−0.6 (5)	0.4 (4)
C_{23}	4.9 (7)	5.8 (7)	3.9 (5)	−0.5 (6)	0.9 (5)	0.7 (5)
O_{23}	11.8 (9)	5.7 (5)	6.8 (6)	4.8 (6)	2.6 (5)	0.4 (5)
C_{31}	4.0 (7)	5.7 (7)	6.3 (7)	0.2 (5)	0.5 (6)	−0.7 (6)
O_{31}	3.1 (5)	12.4 (9)	14. (1)	1.1 (5)	3.8 (6)	0.4 (8)
C_{32}	5.3 (7)	4.6 (6)	5.4 (7)	−0.1 (5)	−1.2 (6)	−0.1 (5)
O_{32}	11.8 (9)	5.8 (5)	6.3 (5)	1.0 (5)	−3.6 (6)	1.2 (4)
C_{33}	4.4 (7)	5.5 (8)	4.9 (7)	0.1 (6)	1.7 (5)	0.3 (6)
O_{33}	11.0 (9)	4.4 (5)	10.5 (8)	−1.9 (6)	1.2 (7)	0.4 (5)

[a] These anisotropic thermal parameters have units of $Å^2$. They enter the expression for the structure factor in the form $\exp[-0.25(B_{11}h^2a^{*2} + B_{22}k^2b^{*2} + B_{33}l^2c^{*2} + 2B_{12}hka^*b^* + 2B_{13}hla^*c^* + 2B_{23}klb^*c^*)]$.

Table VII. Interatomic Distances in $Ru_3H(CO)_9(C_7H_4NS_2)$ with Esd's in Parentheses (Å)

Metal-Metal Bonds			
Ru_1-Ru_2	2.836 (5)	Ru_2-Ru_3	2.798 (6)
Ru_1-Ru_3	2.786 (5)		
Metal-Ligand Bonds			
Ru_1-S_1	2.405 (5)	Ru_3-N	2.177 (9)
Ru_2-S_1	2.404 (5)		
Bonds Involving Ligand Atoms			
S_1-C_1	1.73 (1)	C_5-C_6	1.33 (4)
C_1-N	1.30 (1)	C_6-C_7	1.35 (4)
C_1-S_2	1.73 (1)	C_7-C_2	1.38 (2)
S_2-C_2	1.75 (1)	C_4-H_4	1.2 (2)
N-C_3	1.39 (1)	C_5-H_5	0.6 (2)
C_2-C_3	1.39 (2)	C_6-H_6	1.0 (4)
C_3-C_4	1.40 (2)	C_7-H_7	0.9 (2)
C_4-C_5	1.37 (2)		
Bonds Involving Axial Carbonyls			
Ru_1-C_{11}	1.89 (2)	C_{11}-O_{11}	1.13 (2)
Ru_2-C_{21}	1.90 (2)	C_{21}-O_{21}	1.10 (2)
Ru_3-C_{31}	1.89 (2)	C_{31}-O_{31}	1.12 (2)
Bonds Involving Equatorial Carbonyls			
Ru_1-O_{12}	1.94 (2)	C_{12}-O_{12}	1.16 (2)
Ru_1-C_{13}	1.90 (2)	C_{13}-O_{13}	1.13 (1)
Ru_2-C_{22}	1.95 (1)	C_{22}-O_{22}	1.14 (1)
Ru_2-C_{23}	1.89 (2)	C_{23}-O_{23}	1.15 (2)
Ru_3-C_{32}	1.95 (1)	C_{32}-O_{32}	1.11 (1)
Ru_3-C_{33}	1.91 (2)	C_{33}-O_{33}	1.16 (2)

Table VIII. Principal Bond Angles in $Ru_3H(CO)_9(C_7H_4NS_2)$ with Esd's in Parentheses (deg)

Metal Triangle Angles			
Ru_2-Ru_1-Ru_3	59.7 (1)	Ru_2-Ru_3-Ru_1	61.0 (1)
Ru_1-Ru_2-Ru_3	59.3 (1)		
Sulfur Bridge Angles			
Ru_1-S-Ru_2	72.3 (2)	S-Ru_2-Ru_1	53.9 (1)
S-Ru_1-Ru_2	53.9 (1)		
Metal Surrounding Angles			
S_1-Ru_1-Ru_2	53.9 (1)	C_{11}-Ru_1-C_{12}	94.9 (5)
S_1-Ru_1-Ru_3	80.0 (1)	C_{11}-Ru_1-C_{13}	94.0 (5)
S_1-Ru_1-C_{12}	93.0 (4)	C_{12}-Ru_1-C_{13}	97.4 (5)
S_1-Ru_1-C_{13}	97.2 (4)	C_{13}-Ru_1-Ru_3	86.0 (4)
C_{11}-Ru_1-Ru_2	111.6 (4)	C_{12}-Ru_1-Ru_2	114.1 (4)
C_{11}-Ru_1-Ru_3	91.6 (4)		
S_1-Ru_2-Ru_1	53.9 (1)	C_{21}-Ru_2-C_{22}	91.2 (6)
S_1-Ru_2-Ru_3	79.7 (1)	C_{21}-Ru_2-C_{23}	89.6 (6)
S_1-Ru_2-C_{22}	93.3 (4)	C_{22}-Ru_2-C_{23}	101.9 (6)
S_1-Ru_2-C_{23}	98.7 (4)	C_{23}-Ru_2-Ru_3	86.6 (4)
C_{21}-Ru_2-Ru_1	115.6 (4)	C_{22}-Ru_2-Ru_1	110.6 (4)
C_{21}-Ru_2-Ru_3	94.5 (4)		
N-Ru_3-Ru_1	88.0 (3)	C_{31}-Ru_3-C_{32}	92.1 (7)
N-Ru_3-Ru_2	88.7 (3)	C_{31}-Ru_3-C_{33}	91.9 (6)
N-Ru_3-C_{32}	91.5 (5)	C_{32}-Ru_3-C_{33}	102.6 (6)
N-Ru_3-C_{33}	89.4 (5)	C_{33}-Ru_3-Ru_2	99.7 (4)
C_{31}-Ru_3-Ru_1	89.4 (4)	C_{32}-Ru_3-Ru_1	96.7 (4)
C_{31}-Ru_3-Ru_2	87.1 (4)		
Mercaptobenzothiazole Angles			
Ru_1-S_1-C_1	105.0 (4)	C_1-S_2-C_2	89.0 (6)
Ru_2-S_1-C_1	105.1 (4)	S_2-C_2-C_3	110.2 (9)
Ru_3-N-C_1	118.3 (7)	C_2-C_3-N	113 (1)
Ru_3-N-C_3	128.7 (7)	C_2-C_3-C_4	120 (1)
S_1-C_1-N	124.4 (8)	C_3-C_4-C_5	115 (2)
S_1-C_1-S_2	120.7 (6)	C_4-C_5-C_6	125 (2)
S_2-C_1-N	114.8 (8)	C_5-C_6-C_7	120 (2)
C_1-N-C_3	113.0 (9)		

factors is available as supplementary material.

Results and Discussion

Complex I: $Ru_3H(CO)_{10}(SCH_2COOH)$. As shown in Figure 1, this complex reveals the prevailing reactivity of the sulfur atom toward the metal triangle: the ligand's action on $Ru_3(CO)_{12}$ results in substitution of two axial carbonyls by a symmetric sulfur bridge, while the carboxylic group remains inactive, far from the metal triangle. Figure 2 shows the molecular packing within the unit cell; no hydrogen bond connects the carboxylic group to other molecules, since normal

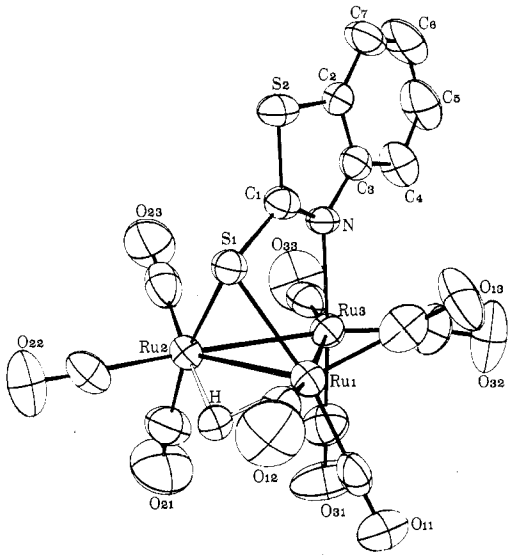

Figure 6. Geometry and labeling of $HRu_3(CO)_9(C_7H_4NS_2)$.

van der Waals distances are observed.

Let us first discuss the structural effect of the sulfur bridge. The molecular unit consists of a triangular array of metal atoms with nearly identical metal–metal bond lengths: Ru_1–Ru_2 = 2.839 (4) Å (supporting bridges), Ru_1–Ru_3 = 2.839 (4) Å, and Ru_2–Ru_3 = 2.826 (5) Å. Some previous structure determinations established that unsupported bridging hydride ligands usually lengthen the corresponding metal–metal bond: $H_2Os_3(CO)_{11}$, 2.90 → 2.98 Å;[13] $H_2Os_3(CO)_{10}(PPh_3)$, 2.89 → 3.02 Å;[15] $H_2Re_3(CO)_{12}^-$, 3.04 → 3.17 Å.[18] Churchill et al. found that a carbido bridge in addition to the bridging hydride leads to a slight shortening of the metal–metal bond:[7] $HRu_3(CO)_{10}(C{=}NMe_2)$, 2.83 → 2.80 Å. Comparison with our result shows that the metal–metal bond length is also influenced by the nature of the bridging ligand in addition to the hydride, since the resulting effect of sulfur and hydride is a retention of the initial bond length. The constraint brought about by the sulfur bridge results in (1) a significant decrease in isotropic thermal parameters of Ru_1 and Ru_2 with respect to Ru_3 [$B(Ru_1)$ = 2.52 (2), $B(Ru_2)$ = 2.56 (2), $B(Ru_3)$ = 2.90 (2) Å^2] and (2) unusual angles on sulfur [Ru_1–S–Ru_2 = 73.0 (1)°] and on ruthenium [S–Ru_1–Ru_2 = 53.5 (1)°, S–Ru_2–Ru_1 = 53.5 (1)°]. This suggests that a reorientation of the metal surrounding is necessary to preserve an octahedral basis set of orbitals on both ruthenium atoms. It can be achieved by rotation around Ru_1–Ru_3 and Ru_2–Ru_3 axes, respectively. Evidence of this move is given by the new positions of the carbonyl ligands perpendicular to these axes with respect to $Ru_3(CO)_{12}$. A projection in the plane of the sulfur bridge (Figure 3) shows that the concerned carbonyls are tilted away from their initial axial or equatorial position. These observations would suggest a "bent" Ru_1–Ru_2 bond, with an orbital overlap which should be maximum under the metal triangle plane. This would favor the insertion of the hydride ligand without further elongation of the metal–metal distance. Indeed, the approximate position of the hydride electronic density is found trans to $C_{13}O_{13}$ and $C_{23}O_{23}$ at a distance of ca. 1.85 Å of both metal atoms.

These observations are in agreement with the occurrence of a "closed" M–H–M system[7,9] (two-electron, three-center bond).

Although the sulfur bridge influence seems quite large on the distortion of the molecule, a slight perturbation can be assigned to the hydride ligand. Its presence between the four carbonyls $C_{11}O_{11}$ and $C_{21}O_{21}$ (axial) and $C_{12}O_{12}$ and $C_{22}O_{22}$ (equatorial) has a small stereochemical influence on their orientations. For axial carbonyls, it is mixed with the influence of sulfur. For equatorial carbonyls, the following slight perturbations are observed (Figure 4): Adjacent angles C_{12}–Ru_1–Ru_2 (114.9°) and C_{22}–Ru_2–Ru_1 (115.6°) are both 17° larger than the mean value 97.9° observed in $Ru_3(CO)_{12}$.[19] This stereochemical influence is transmitted to adjacent carbonyls $C_{13}O_{13}$ and $C_{23}O_{23}$ and results in a reduction of the following angles: C_{12}–Ru_1–C_{13} = 100.3°, C_{22}–Ru_2–C_{23} = 95.1°, compared to a mean value in $Ru_3(CO)_{12}$ of 104.1°; C_{13}–Ru_1–Ru_3 = 85.6°, C_{23}–Ru_2–Ru_3 = 87.1°, compared to a mean value in $Ru_3(CO)_{12}$ of 97.9. These distortions are related to the presence of the hydride ligand. Indeed, they are also observed in the molecule $H_2Os_3(CO)_{11}$[13] in which the bridging hydride is the only one to have such a possible influence in the molecule.

Thus, the present complex is in agreement with the model proposed by Lewis et al.[6] for thiol reaction on $Ru_3(CO)_{12}$. A brief structural report on $HOs_3(CO)_{10}(SEt)$[20] shows that a similar reaction occurs with $Os_3(CO)_{12}$. In contrast, the reaction involving $Fe_3(CO)_{12}$ was shown to give nonacarbonyl derivatives of stoichiometry $HFe_3(CO)_9SR$, with a triply bridging sulfur, recently confirmed by an X-ray structure determination.[12] Bau et al. found unusual short iron–sulfur distances in that compound, while the ruthenium–sulfur distance in our complex (2.387, 2.388 Å) is only a little bit shorter than the usual Ru–S in a nonbridged mononuclear species [$Ru(mbt)_2(CO)_2(py)_2$: 2.406 Å].[5] A direct comparison of Ru–S and Fe–S bonds can be made by an approximate

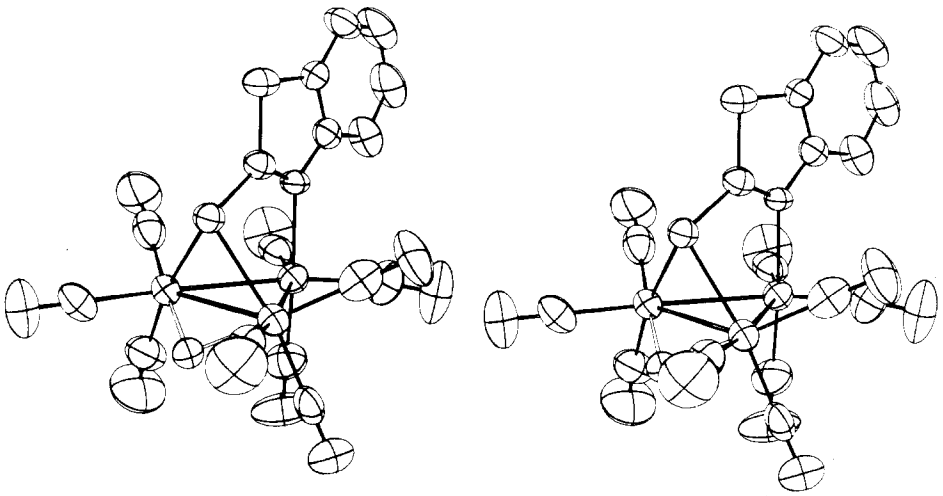

Figure 7. Stereoscopic view of $HRu_3(CO)_9(C_7H_4NS_2)$.

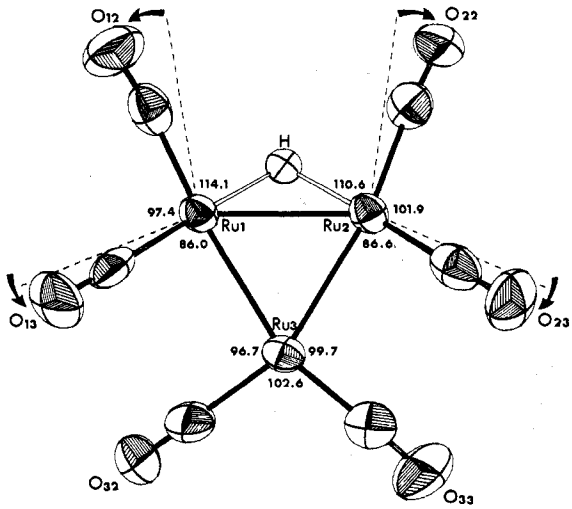

Figure 8. Stereochemical influence of the bridging hydride: equatorial distribution of carbonyl ligands in $HRu_3(CO)_9(C_7H_4NS_2)$ with respect to $Ru_3(CO)_{12}$.

evaluation of covalent radii of sulfur from the mean value of M–M and M–S bonds: $r_S = 0.81$ in $HFe_3(CO)_9SR$, $r_S = 0.98$ in $HRu_3(CO)_{10}SR$.

It might be tempting to relate the smaller covalent radii to an increased strength in the metal–sulfur bond if the bonds were really linear. However, the triangular geometries in bridged species are not consistent with linear orbital overlap between sulfur and octahedral metals. Thus, the constitution of molecular orbitals between metal and sulfur is made by a necessarily lateral overlap, the magnitude of which has a prevailing influence on the bond strength. In both cases, the carbonyl ligands trans to sulfur exhibit an angle with the metal–sulfur direction, showing a more lateral overlap in the iron derivative: S–Ru–C(axial) = 166.6°, 169.7°; S–Fe–C(axial) = 145.2°, 142.4°. Let us remark that the value of this angle is influenced by metal–ligand bond strength. Ignoring metal–metal interactions, a more lateral overlap would indicate a decrease in the bond strength. This is in agreement with the weaker stability of the triply bridging species.

Following these observations, the μ_2-S is more likely to correspond to the surface complex. Such an overlap, more or less lateral, is of main interest for metal surface protection: the sulfur bridge can thus accomodate variable metal–metal distances which can occur on the surface. The possibility of a μ_3-S cannot be excluded but may be of weaker stability.

Complex II: $Ru_3H(CO)_9(C_7H_4NS_2)$. The crystal consists of discrete molecular units of $Ru_3H(CO)_9(C_7H_4NS_2)$ separated by normal van der Waals distances. Figure 5 shows molecular packing within the unit cell. Figures 6 and 7 reveal the unusual linkage of mercaptobenzothiazole: coordination is made on Ru_1 and Ru_2 through the exocyclic bridging sulfur and on Ru_3 through the nitrogen atom. The mean plane of mercaptobenzothiazole is roughly a mirror plane for the whole molecule.

This is a rare example of thioamide coordination to $Ru_3(CO)_{12}$. Comparison with the previous example of thiol coordination shows a similar structure of the sulfur bridge (Ru_1–S = 2.405 (5), Ru_2–S = 2.404 (5) Å), while the corresponding metal–metal bond Ru_1–Ru_2 = 2.836 (5) Å is identical with the previous value of 2.839 (5) Å within experimental error. The resulting deformations of metal surrounding are the same as described in the first case. Moreover, a similar influence of the hydride ligand on equatorial carbonyls is observed (Figure 8). It is also noteworthy that the nitrogen atom does not disturb the carbonyl arrangement around Ru_3. Although the main deformations are the same as in the previous structure, a slight difference is observed in the metal triangle. Considering the value of unsupported metal–metal bond lengths in $Ru_3H(CO)_{10}(SCH_2COOH)$ (Ru_1–Ru_3 = 2.839 (5), Ru_2–Ru_3 = 2.826 (5) Å), the same bonds are found significantly shorter in the new complex (Ru_1–Ru_3 = 2.786 (5), Ru_2–Ru_3 = 2.798 (6) Å). This effect can be related to a particular influence of the SCN bridge.

Let us now discuss the molecular structure of the ligand. It can exist as a free molecule under two tautomeric forms HN—C=S and N=C—SH in a thione–thiol equilibrium. A wide range of coordination compounds involving mercaptobenzothiazole and closely related thioamides[21-24] gave evidence of both possibilities. In the solid state, the molecule was shown to be dimeric, and hydrogen bonded, with S–C = 1.66 Å and C–N = 1.35 Å.[25] These distances are intermediate between single and double bond lengths, which suggests some π electron delocalization along the N···C···S group.

In the complex, the exocyclic sulfur atom has the same behavior as the thiol function in mercaptoethanoic acid. The tetrahedral geometry strongly suggests a true thiolate form requiring location of π electrons between carbon and nitrogen. Indeed, a significant shortening of the NC bond (1.35 → 1.30 Å) occurs together with a planar-trigonal nitrogen, while the S–C bond is simultaneously elongated (1.66 → 1.73 Å) with respect to the free ligand.

Excluding carbonyl ligands, such a capped structural arrangement provides a complete metal protection which should be of main interest for metal surface inhibition. The value of the present model was checked by comparison of its infrared spectra with the corresponding reflection spectra of the actual surface complex.[3] Such a comparison requires an understanding of the infrared spectra of the free ligand. However, the assignment of infrared bands in thioamides has been a matter of considerable controversy due to the occurence of mixed vibrations.[26-31] Thus, it should not be correct to use straightforwardly and without care the concept of characteristic bond frequency. In this respect, the nomenclature proposed by Jensen and Nielsen[28] seems satisfactory.

Table IX contains infrared spectra of the free ligand and the following complexes: (a) $[Mn(CO)_3(C_7H_4NS_2)]_2$,[21] (b) $[Re(CO)_3(C_7H_4NS_2)]_2$,[21] (c) $Ru_3H(CO)_9(C_7H_4NS_2)$ (this work), and (d) a surface complex (copper inhibition).[3] Our discussion is limited to the study of the most characteristic shifts resulting from simultaneous S and N coordination with the support of X-ray structures showing the arrangements:

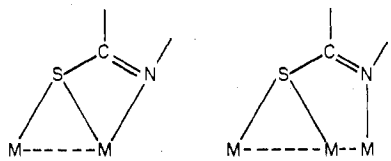

Table IX suggests two general observations: (1) It is not possible to distinguish structures A and B only on the basis of infrared spectra. (2) The shifts observed in a, b, and c complexes are nearly the same as in the reflection spectra for d, which suggests either structure A or structure B for the surface complex.

A more detailed study of the observed shifts would be of interest for infrared assignments: NCS group vibrations should be the most sensitive to coordination. Although the increased double-bond character of CN would result in a shift of ν(CN) to higher frequency, coordination through nitrogen would also result in a frequency decrease of the same band. It is, thus, difficult to determine which of the two effects will be prevailing. Moreover, the CN vibration in free thioamides participates to several bands[28] and is initially coupled with the NH deformation. Therefore, the C=N vibration in our complexes is no longer comparable with the initial vibrations

Table IX. Infrared Spectra[a] of Free Ligand and Complexes (cm^{-1})

	Complexes			
Free ligand Hmbt[b]	a[c] $[Mn(CO)_3(mbt)]_2$	b[c] $[Re(CO)_3(mbt)]_2$	c $Ru_3H(CO)_9(mbt)$	d Surface complex
1604 ms				
	1570 m	1575 m	1565 w	1565 w
1505 s				
1464 ms	1465, 1455 ms	1470, 1460 ms	1458 s	1458 m
1433 s	1412 s	1412 s	1417 ms	1410 s
1328 s	1323 w	1325 w	1321 m	1315 w
1290 ms	1290 w	1297 w	1275 vw	
1251 ms	1260 w	1262 w	1240 ms	1245 m
1159 w	1163 vw	1170 vw	1158 vw	
1144 w				
1132 w	1133 w	1138 vw		
1080 s	1092 s, 1082 s	1105 s, 1094 s	1105 vw, 1092 s	1080 m
1040 s	1040 s	1045 s	1035 s	1020 s
1019 s	1019 s	1020 ms	1018 ms	1010 s
1002 sh				
984 sh	980 vw	985 vw		
940 w	940 w	948 w	940 w	930 w
869 w	890 vw	900 vw	870 vw	
856 w			852 w	
850 w	850 w	858 vw		
753 s	758 s	762 s	760 s	750 s
720 sh	725 ms	728 ms	730 ms	725, 720 m
709 sh	702 ms	702 ms	708 ms	700 w
672 s	673 s	648 s	635 ms	670 w
	626 s	628 s	612 ms	
607 m			590 s	
570 m			580 s	
524 w	528 m	535 m		

[a] s = strong, sh = shoulder, ms = medium strong, m = medium, mw = medium weak, w = weak, vw = very weak. [b] Hmbt is mercaptobenzothiazole. [c] The IR spectra of Mn and Re complexes were erroneously reversed by the editor in the previous paper (ref 21).

in the free ligand. Indeed, the infrared spectra in the range 1600–1400 cm^{-1} appear completely different:

The strong absorption at 1600 cm^{-1} disappears upon complexation.

A new band, of weak to medium intensity, appears in the range 1560–1570 cm^{-1} and can be assigned to a major ν(C=N) contribution in agreement with several authors.[29,30]

The "B" band (Jensen and Nielsen nomenclature[28]) disappears in all cases. This absorption seems the most characteristic of the HN—C=S group. It has a prevailing CN character, probably mixed with δ(NH) as shown by deuteration studies.[27,28] Its total disappearance is a diagnosis probe of nitrogen coordination when the molecule is under the thiolate form. Its absence was also found characteristic by Dehand and Jordanov,[30] while a coordination without hydrogen departure would have only a weak influence on this band.[31]

The band at 1433 cm^{-1} exhibits in all cases a characteristic shift of ca. 20 cm^{-1} to lower frequencies.

In the range 1300–900 cm^{-1}, Rao and Venkataraghavan[26] noted the difficulty of any specific assignment for mercaptobenzothiazole. In this region, a strong absorption at 1077 cm^{-1} is sometimes assigned to a C=S vibration.[27] However, its position and intensity in the complexes (1090–1080 (s) cm^{-1}) is not consistent with the SC single-bond character found in X-ray structures. Moreover, Jensen and Nielsen[28] showed that the spectra of sulfur and selenium derivatives in thioamides and selenoamides were virtually superimposable in this region and concluded the absence of ν(C=S) in thioamides. Thus, the CS vibration has a predominant single-bond character and should be found in the 600–800 range. As shown by Dehand and Jordanov, the band at 670 cm^{-1} which has some ν(CS) contribution exhibits a frequency and intensity decrease upon S complexation. However, the occurrence of metal–carbonyl vibrations in the same region may prevent the use of this band as a diagnosis probe in carbonyl species. Indeed, the strong absorption at 670 cm^{-1} in the manganese complex a has its equivalent at 648 cm^{-1} in the isomorphous rhenium complex b. Since this band is the lone difference between a and b, the lowest frequency in the case of the heavier atom is proving metal participation in the vibration. In spite of this difficulty, the importance of the exocyclic sulfur in metal surface protection is clearly demonstrated. Moreover, benzothiazole, which has no exocyclic sulfur, is a poor corrosion inhibitor.

Acknowledgment. The authors thank Mrs. C. Deltcheff for the careful recording of infrared spectra. This work was generously supported by the Delegation Generale à la Recherche Scientifique (Contract No. 75-7-0001).

Registry No. I, 66515-96-6; II, 66515-97-7; $Ru_3(CO)_{12}$, 15243-33-1.

Supplementary Material Available: Listings of observed and calculated structure factors in $Ru_3H(CO)_{10}(SCH_2COOH)$ and $Ru_3H(CO)_9(C_7H_4NS_2)$ (36 pages). Ordering information is given on any current masthead page.

References and Notes

(1) Proceedings of the 4th European Symposium on Corrosion Inhibitors, Ferrara, Italy, Sept 15–19, 1975.
(2) R. Mason, *Pure Appl. Chem.*, **33**, 513–526 (1973).
(3) S. Thibault and J. Talbot, *Bull. Soc. Chim. Fr.*, 1348 (1972), and personal communication of a new spectra.
(4) S. Jeannin, Y. Jeannin, and G. Lavigne, *Transition Met. Chem.*, **1**, 186–191 (1976).
(5) S. Jeannin, Y. Jeannin, and G. Lavigne, *Transition Met. Chem.*, **1**, 192–195 (1976).
(6) G. R. Grooks, B. F. G. Johnson, J. Lewis, and I. G. Williams, *J. Chem. Soc. A*, 797 (1976).
(7) M. R. Churchill, B. G. DeBoer, and F. J. Rotella, *Inorg. Chem.*, **15**, 1843–1853 (1976).
(8) D. T. Cromer and J. B. Mann, *Acta Crystallogr., Sect. A*, **24**, 321 (1968). See also "International Tables for X-ray Crystallography", Vol. IV, Kynoch Press, Birmingham, England, 1975.
(9) R. Bau and T. F. Koetzle, *J. Am. Chem. Soc.*, in press.
(10) S. M. Kirtley, J. P. Olsen, and R. Bau, *J. Am. Chem. Soc.*, **95**, 4532–4536 (1973).
(11) G. M. Sheldrick and J. P. Yesinowski, *J. Chem. Soc., Dalton Trans.*, 873–876 (1975).
(12) R. Bau, B. Don, R. Greatrex, R. J. Haines, R. A. Love, and R. D. Wilson, *Inorg. Chem.*, **14**, 3021–3025 (1975).
(13) M. R. Churchill and B. G. DeBoer, *Inorg. Chem.*, **16**, 878–884 (1977).
(14) M. R. Churchill and B. G. DeBoer, *Inorg. Chem.*, **16**, 1141–1146 (1977).
(15) M. R. Churchill and B. G. DeBoer, *Inorg. Chem.*, **16**, 2397–2403 (1977).
(16) S. J. LaPlaca and J. A. Ibers, *Acta Crystallogr.* **18**, 511 (1965).
(17) C. K. Johnson, Report No. 3794, Oak Ridge National Laboratory, Oak Ridge, Tenn., 1965.
(18) M. R. Churchill, P. M. Bird, H. D. Kaesz, R. Bau, and B. Fontal, *J. Am. Chem. Soc*, **90**, 7135 (1968).
(19) M. R. Churchill, F. J. Hollander, and J. P. Hutchinson, **16**, 2655 (1977).
(20) R. Mason, Special Lecture, XXIIIrd IUPAC Congress, Boston, Mass., July 26–30, 1971, Vol. 6, p 31.
(21) S. Jeannin, Y. Jeannin, and G. Lavigne, *Transition Met. Chem.*, **1**, 195–199 (1976).
(22) S. Jeannin, Y. Jeannin, and G. Lavigne, *J. Cryst. Mol. Struct.*, in press.
(23) C. C. Ashworth, N. A. Bailey, M. Johnson, J. A. McCleverty, N. Morrisson, and B. Tabbiner, *J. Chem. Soc., Chem. Commun.*, 743 (1976).
(24) R. Alper and A. S. K. Chan, *Inorg. Chem.*, **13**, 225–232 (1974).
(25) J. P. Chesick and J. Donohue, *Acta Crystallogr., Sect. B*, **27**, 1441 (1971).
(26) C. N. R. Rao and R. Venkataraghavan, *Spectrochim. Acta*, **18**, 541–547 (1962).
(27) H. Larivé, A. J. Chambonnet, and J. Metzger, *Bull. Soc. Chim. Fr.*, 1675 (1963).
(28) K. A. Jensen and P. H. Nielsen, *Acta Chem. Scand.*, **20**, 597–629 (1966), and references therein.
(29) J. P. Favre, *Bull. Soc. Chim. Fr.*, 1572–1582 (1967).
(30) J. Dehand and J. Jordanov, *Inorg. Chim. Acta*, **17**, 37–44 (1976).
(31) C. Preti and G. Tosi, *J. Inorg. Nucl. Chem.*, **38**, 1125–1129 (1976).